AIP | Applied Physics Letters

Designing one dimensional Co-Ni/Co3O4-NiO core/shell nano-heterostructure electrodes for high-performance pseudocapacitor

Ashutosh K. Singh, Debasish Sarkar, Gobinda Gopal Khan, and Kalyan Mandal

Citation: Applied Physics Letters **104**, 133904 (2014); doi: 10.1063/1.4870628
View online: http://dx.doi.org/10.1063/1.4870628
View Table of Contents: http://scitation.aip.org/content/aip/journal/apl/104/13?ver=pdfcov
Published by the AIP Publishing

Designing one dimensional Co-Ni/Co_3O_4-NiO core/shell nano-heterostructure electrodes for high-performance pseudocapacitor

Ashutosh K. Singh,[1,a),b)] Debasish Sarkar,[1,2,b),c)] Gobinda Gopal Khan,[3,b),d)] and Kalyan Mandal[1,e)]
[1]*Department of Condensed Matter Physics and Material Sciences, S. N. Bose National Centre for Basic Sciences, Block JD, Sector III, Salt Lake City, Kolkata 700 098, India*
[2]*Solid State and Structural Chemistry Unit, Indian Institute of Science, Bangalore 560012, India*
[3]*Centre for Research in Nanoscience and Nanotechnology, University of Calcutta, Technology Campus, Block JD2, Sector III, Salt Lake City, Kolkata 700 098, India*

(Received 12 March 2014; accepted 25 March 2014; published online 4 April 2014)

A high-performance supercapacitor electrode based on unique 1D Co-Ni/Co_3O_4-NiO core/shell nano-heterostructures is designed and fabricated. The nano-heterostructures exhibit high specific capacitance (2013 F g^{-1} at 2.5 A g^{-1}), high energy and power density (23 Wh kg^{-1} and 5.5 kW kg^{-1}, at the discharge current density of 20.8 A g^{-1}), good capacitance retention and long cyclicality. The remarkable electrochemical property of the large surface area nano-heterostructures is demonstrated based on the effective nano-architectural design of the electrode with the coexistence of the two highly redox active materials at the surface supported by highly conducting metal alloy channel at the core for faster charge transport. © *2014 AIP Publishing LLC*. [http://dx.doi.org/10.1063/1.4870628]

Supercapacitors (SCs) have drawn immense attention as the promising candidates for the next generation power sources in portable electronics because of their higher power density, faster charge/discharge process, and longer lifetime; complementary to the energy storage devices, such as rechargeable batteries and fuel cells.[1–3] Recently, redox-active transition-metal oxides (TMOs) such as RuO_2, MnO_2, Fe_2O_3, NiO, and Co_3O_4 are demonstrated as the emerging electrode materials for pseudocapacitors because of their high specific capacitances and excellent reversibility arising from the fast and reversible Faradaic reactions.[1,2] Although the poor conductivity, poor cycling stability, and sometimes high cost (for RuO_2) have become the challenging concerns to fabricate transition-metal oxide based pseudocapacitors.[1] In this context, selection of specific materials as well as the proper nano-engineering design of the electrode are very effective to fabricate high performance SCs. As the high cost of RuO_2 limits its practical applications, among the other TMOs, Co_3O_4, and NiO could have been ideal alternative for the SCs electrode because of their high theoretical capacitances (3560 and 2573 F g^{-1}, respectively), availability, stability, and relatively low cost. It is also well studied that the nano-architectures with large active surface area, short ion transport pathway, and good electronic conductivity could improve the performance of SCs. In this backdrop, recently, 1D hybrid nanostructures based on Co_3O_4 and NiO and their mixed and complex oxides (binary and ternary) have been demonstrated as the promising SCs electrodes.[4–15] Still there are ample opportunities to go for the effective nano-engineering design of the SC electrodes based on Co_3O_4 and NiO in a most facile way with remarkably improved performance.

Here, we report the electrochemical properties of the 1D hybrid nano-architecture of Co_3O_4-NiO mixed oxide nano-shell grown on Co-Ni metal alloy core nanowires (i.e., Co-Ni/Co_3O_4-NiO core/shell nano-heterostructures). This unique nano-architecture of the hybrid metal oxides has been chosen as anticipation with the high specific capacitance as well as high energy and power density of the Co_3O_4 and NiO based SCs. The 1D Co-Ni/Co_3O_4-NiO core/shell nano-heterostructures have two different redox active oxides with large active surface to serve as the electrode. The thin mixed-oxide layer will provide the short ion transport path, whereas the metal alloy core will act as the fast electron conducting channel to the current collector.

The electrode containing high density ordered arrays of 1D Co-Ni/Co_3O_4-NiO core/shell nano-heterostructures has been fabricated by controlled high temperature oxidation of Co-Ni alloy nanowires (NWs) grown via template assisted electrodeposition technique by using the highly ordered nanoporous anodic aluminium oxide (AAO) as template, as described elsewhere[15] (see supplementary material[16]). Fig. 1 schematically shows the two-step fabrication of the 1D Co-Ni/Co_3O_4-NiO core/shell nano-heterostructures: (1) electrodeposition of the arrays of Co-Ni NWs in AAO and (2) controlled high temperature oxidation of Co-Ni NWs in air atmosphere. The unique feature of this technique is that individual nano-heterostructure in the electrode has its own contact with the current collector (Au), which results the enhanced charge transfer kinetics.

Fig. 2(a) shows the field emission scanning electron microscopy (FESEM) image of the as-prepared Co-Ni/Co_3O_4-NiO core/shell nano-heterostructures having uniform diameter (~150 nm). Inset of Fig. 2(a) indicates that the surface of nano-heterostructures is very rough and porous compared to that of the Co-Ni NWs (see Fig. S1, supplementary material[16]), which will further increase the active surface area of the electrode. The transmission electron microscopy

a)Email: ashuvishen@gmail.com
b)A. K. Singh, D. Sarkar, and G. G. Khan contributed equally to this work.
c)Email: deb.sarkar1985@gmail.com
d)Author to whom correspondence should be addressed. Electronic mail: gobinda.gk@gmail.com. Tel.: +91 (033) 2335 0067.
e)Email: kalyan@boson.bose.res.in

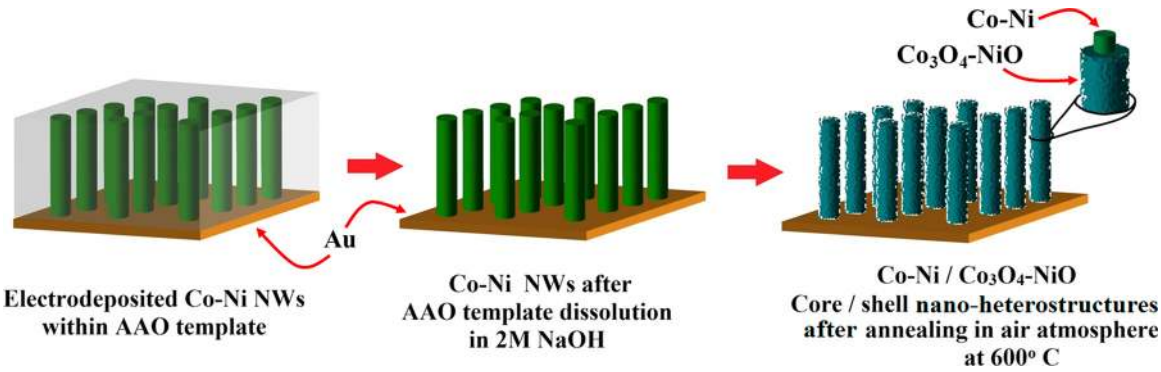

FIG. 1. Schematic overview of the preparation of Co-Ni/Co_3O_4-NiO core/shell nano-heterostructures.

(TEM) [Fig. 2(b)] and energy filtered TEM (EFTEM) [Fig. 2(d)] micrographs of the Co-Ni/Co_3O_4-NiO core/shell nano-heterostructures clearly show the formation the uniform nano-layer (~25–30 nm) of Co_3O_4-NiO on Co-Ni metal alloy core. Formation of a good quality nano-heterostructures with uniform chemical composition is also evident from Fig. 2(d). Selected area electron diffraction (SAED) pattern [inset of Fig. 2(b)] and high resolution TEM (HRTEM) image [Fig. 2(c)] confirm the polycrystalline nature of the nano-heterostructures. The HRTEM micrograph with *d*-spacing of 0.28, 0.14, and 0.24 nm correspond to the (111) NiO, (220) NiO, and (220) Co_3O_4, respectively. The x-ray diffraction pattern of nano-heterostructures also shows its polycrystalline nature (see Fig. S2, supplementary material[16]). The XRD pattern consists of peaks that correspond to the core containing Co and Ni and shell nanolayer which contains NiO and Co_3O_4 and also the metallic Au layer underneath the nano-heterostructures. The energy-dispersive x-ray spectroscopy (EDS) spectrum confirms the presence of Co, Ni, and O in the nano-heterostructures, where the Co:Ni ratio is found to be 1.3:1 in Co_3O_4-NiO mixed oxides (see Fig. S3, supplementary material[16]).

Electrochemical properties of the Co-Ni/Co_3O_4-NiO core/shell nano-heterostructures electrode was studied by cyclic voltammetry (CV) and galvanostatic (GV) charge/discharge method by using a three-electrode system, where the nano-heterostructures as working electrode was dipped in 1M KOH aqueous solution at room temperature. The Ag/AgCl and Pt wire were used as reference and counter electrodes, respectively. Fig. 3(a) shows the CV curves of the as-prepared nano-heterostructures, recorded at different scan rates (2–100 mV s^{-1}) within the voltage window of 0.1–0.5 V. Each CV loop characterized by oxidation and reduction peaks demonstrates the pseudocapacitive behaviour of the nano-heterostructures, which is quite different from the rectangular CV loops owing to the formation of Helmholtz layer in electrical double layer capacitors (EDLCs). The redox peaks observed for all scan rates are associated with the surface or near surface based Faradic reactions as governed by the equations:[1,10] $Co_3O_4 + H_2O + OH^- \leftrightarrow 3CoOOH + e^-$ and $NiO + OH^- \leftrightarrow NiOOH + e^-$. The charging process involves the oxidation of Co^{2+} and Ni^{2+} into Co^{3+} and Ni^{3+}, respectively, with the movement of the corresponding electrons towards the current collector (Au) through the electrode; while discharging involves subsequent reduction of metal ions from +3 oxidation state to +2 state followed by the electron transport in reverse direction. Good kinetic reversibility characteristics of the electrode are confirmed from the highly symmetric nature of the redox peaks of the CV curves taken at different scan rates.[17,18] This observation also reveals the high cyclability of the electrode. The increase of current with increasing scan rate is quite obvious because during the fast scanning, the diffusion layer cannot extend far from the electrode surface, thus facilitating higher electrolyte flux towards the electrode leading to higher value of current which is in contrary to the case at lower scan rates where the large width of the diffusion layer significantly reduces the electrolyte flux and hence the current. However, the linear relation between the peak current (*I*) of CV loops and the square root of scan rate ($f^{1/2}$) observed for nano-heterostructures at different scan rates (see Fig. S4, supplementary material[16]) demonstrates the fast electron transfer during redox reactions, indicating the superior performance of the nano-heterostructures as SC electrode.[19] This high rate performance can be attributed to the rough and porous structure of the electrode materials which can store the electrolytic ions effectively to facilitate ion movement and also shortens the ion diffusion path to the interiors of the electrode even at higher scan rates.

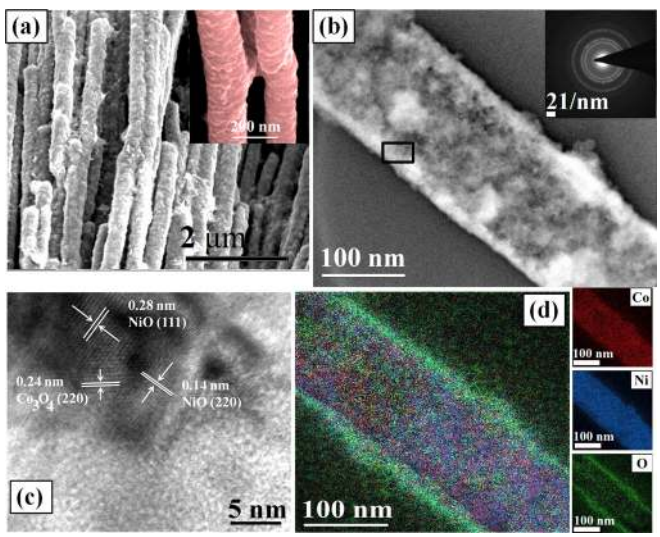

FIG. 2. (a) and inset of (a): FESEM micrographs, (b) TEM and SAED pattern (inset of (b)), (c) HRTEM image, and (d) EFTEM micrographs of the Co-Ni/Co_3O_4-NiO core/shell nano-heterostructures.

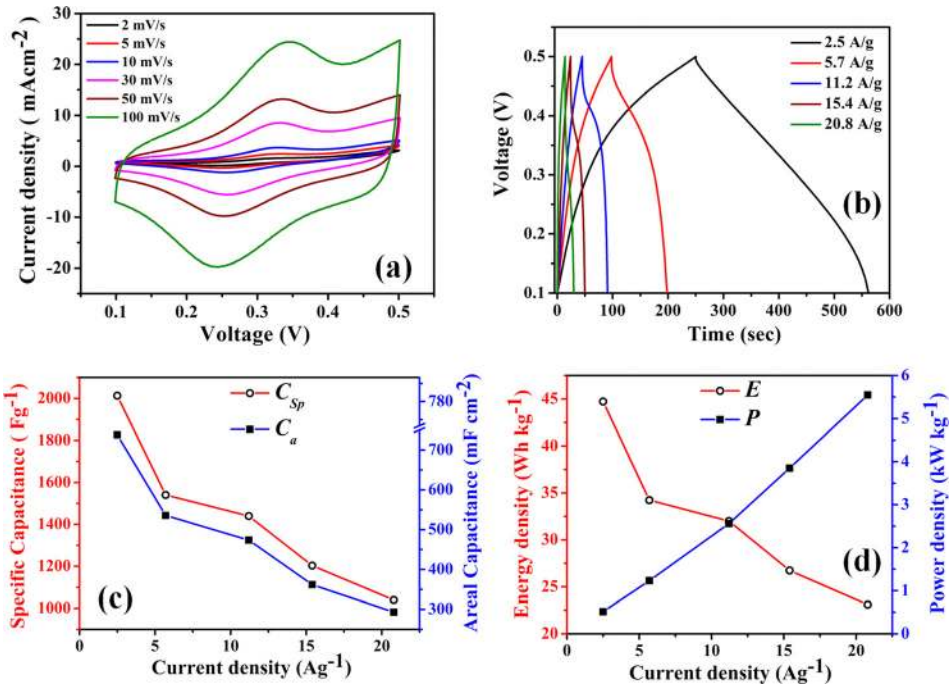

FIG. 3. (a) Cyclic voltammograms of the nano-heterostructures electrode recorded at different scan rates. (b) Galvanostatic charge/discharge curves of the nano-heterostructures electrode recorded at different constant current densities. (c) Areal capacitance and specific capacitance calculated from the charge/discharge curves as a function of current density. (d) Variation of power density and energy density of the nano-heterostructures as a function of current density.

Fig. 3(b) shows the typical constant current GV charge/discharge curves of the nano-heterostructures electrode at different current densities (2.5–21 A g^{-1}) within the voltage window of 0.1–0.5 V. The symmetric nature of the curves suggests excellent electrochemical characteristics of the nano-heterostructures manifested by reversible redox reactions. All the charge/discharge curves of the nano-heterostructures exhibit low IR drop which can be attributed to the special core/shell design of the electrode material and also due to the binder-free direct contact of nano-heterostructures with the current collector that significantly reduces the interfacial resistance. The symmetric nature of the cycling curves remains unaltered even when the current density reaches as high as 21 A g^{-1}, which indicates very high rate stability of the electrode. From the discharging curves, the specific and areal capacitances are calculated by the formulas, $C_{sp} = I\Delta t/m\Delta V$ and $C_a = I\Delta t/a\Delta V$, respectively (where I is the discharge current, Δt is the discharging time, ΔV is the potential window excluding the IR drop region, m is the mass of the active material, i.e., the total mass of the nano-heterostructures, here loading density of nano-heterostructures is 0.376 mg cm^{-2} and a is the surface area of working electrode) and their variation with current density is shown in Fig. 3(c). Maximum value of C_{sp} of nano-heterostructures electrode is found to be nearly 2013 F g^{-1} at the current density of 2.5 A g^{-1} and the corresponding C_a of the nano-heterostructures electrode is 738 mF cm^{-2} at an equivalent current density of 0.94 mA cm^{-2}. The capacitance of the Co-Ni mixed oxide is found comparable ($NiCo_2O_4$ nanosheet/carbon fabric,[4] Ni-Co oxide NWs/TiO_2[5]) and even much better than the values reported for other such Co/Ni based oxide composites, such as $NiCo_2O_4$ nanorods and nanosheets/carbon fibber,[1] Ni-Co oxides,[6] nanoporous NiO film,[7] mesoporous NiO,[8] spherical porous NiO,[9] mesoporous Co_2O_3 NWs,[10] Co_3O_4 NWs@carbon paper,[11] $NiCo_2O_4$ nano-needle,[12] $NiCo_2O_4$ NWs.[13,14] However, the C_{sp} of the nano-heterostructures remains 1040 F g^{-1} even when the current density increases as high as 20.8 A g^{-1}, implying that it can retain ~51.67% of its initial capacitance when the current density is increased by almost 8.5 times. This high specific capacitance with impressive rate capability, i.e., excellent capacitive performance of the nano-heterostructures is mainly due to the large surface area nano-architectural design of the electrode having good electrochemical utilization of two highly redox active materials together with high electrical conductivity provided by the metal alloy core. Here, the high surface area of the nano-heterostructure electrode (due to the presence of nano-porous oxide shell layer) provides significantly large platform for the fast charge intercalation/deintercalation within the electrode material during the faradic reactions, whereas, the highly conductive core helps for faster electron transport that have been generated through redox reactions, to the current collector, thus promoted relatively high rate capability. Moreover, this thin porous oxide layer facilitates electrolytic ion and electron transport to the interiors of the electrode material, resulting higher electrochemical performance.

The energy and power densities calculated by the formulas, $E = 1/2C_{sp}(\Delta V)^2$ and $P = E/\Delta t$, respectively (where "E (Wh kg^{-1})," "C_{sp} (F g^{-1})," "ΔV (V)," "Δt (s)," and "P (kW kg^{-1})" are the energy density, specific capacitance, potential window of discharge, discharging time, and power density, respectively.) from the charge−discharge curves at different current densities are plotted in Fig. 3(d). The energy density of the nano-heterostructures electrode decreases from 44.7 to 23 Wh kg^{-1}, when the power density for the same increases from 0.5 to 5.6 kW kg^{-1}, as the discharge current density increased from 2.5 to 20.8 A g^{-1}. The nano-heterostructures SC maintains high power density without much reduction in energy density, which is found better than reported previously for: NiO_x,[20] $Ni(OH)_2$,[21] CoO_x,[22] $Co(OH)_2$[23] based SC electrodes.

The nano-heterostructures also exhibit excellent electrochemical cycling stability beyond 3000 cycles carried out at a current density of 2.5 A g^{-1}, with a negligible decay

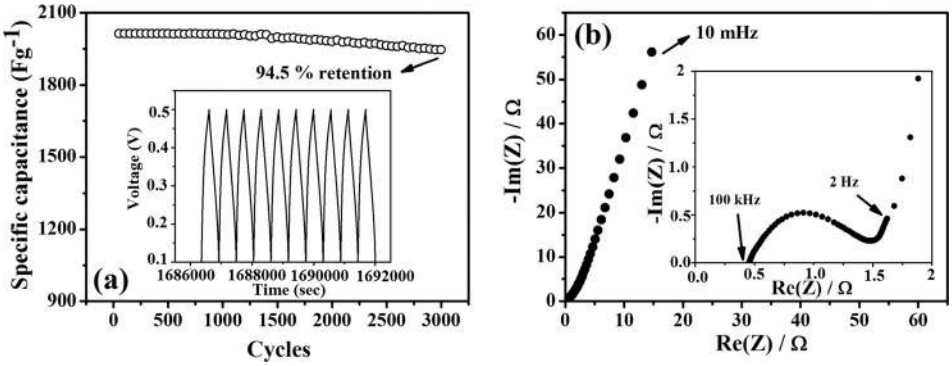

FIG. 4. (a) Cycling performance of nano-heterostructures electrode (3000 charge/discharge cycles at a constant current density of 2.5 A g^{-1}). Inset of (a) last 10 cycles of the charging/discharging curves. (b) Nyquist plot of the EIS data of the nano-heterostructures electrode over the frequency range from 10 mHz to 100 kHz.

(5.5%) of its initial value of C_{sp} [Fig. 4(a)]. From the last 10 charge/discharge cycles shown in Fig. 4(a), it can be seen that the symmetric triangular shape of the charging/discharging profiles remain almost unchanged during the long cycle test which again signifies stable electrochemical performance and efficient charge transport during the reactions. Such high stability of the electrode can be accounted for the higher mechanical integrity which can sustain significant structural distortion during repetitive charging/discharging process and also non-dissolution of active material within the electrolyte. However, small decrease in specific capacitance after 3000 cycles may be due to the swelling of the electrode material owing to the continuous ion insertion/deinsertion process during long cycle test.

The electrochemical impedance spectroscopy (EIS) measurements data of the nano-heterostructures analysed by using Nyquist plot are shown in Fig. 4(b). The finite slope of the impedance spectra ($\theta > 45°$) at lower frequencies indicates Warburg resistance arises from the diffusion of the electrolyte ions within the pores of the nano-heterostructure electrode. The intercept on the real axis in the high frequency region represents the equivalent series resistance (R_s), which includes bulk resistance of electrolyte, intrinsic resistance of active material, and contact resistance of electrode/electrolyte interface. The value of R_s of the nano-heterostructure electrode is calculated as 0.452 Ω, indicates higher electrical conductivity of the electrode, which can be attributed to the presence of Co-Ni alloy core within the nano-heterostructure. The diameter of the semicircle in the high frequency region provides the charge transfer resistance (R_{ct}) resulting from the diffusion of electrons during redox reactions. The low value of R_{ct} of the nano-heterostructures (1.033 Ω) represents its low faradic resistance due to high redox activity of the composite materials indicates easy charge transport across the electrode-electrolyte interface. Therefore, from the EIS analysis it can be understood that this unique core/shell combination of two redox active materials significantly reduces the inherent resistances of the whole electrochemical system leading to enhanced capacitive performance.

In conclusion, 1D Co-Ni/Co_3O_4-NiO core/shell nano-heterostructures with remarkable pseudocapacitance has been demonstrated. The nano-heterostructures are fabricated by combining simple electrochemical deposition of Co-Ni alloy nanowires followed by controlled oxidation. The unique nano-architectural design of the nano-heterostructures electrode having large rough surface area coupled with the presence of two highly redox active materials with short ion diffusion path grown on the highly conducting metal alloy channel facilitating the faster charge transport helps to achieve enhanced electrochemical properties suitable for the supercapacitor applications.

This work was supported by the Board of Research in Nuclear Sciences (BRNS), Government of India funded project 2009/37/16/BRNS. One of the authors, Gobinda Gopal Khan is thankful to the Department of Science and Technology (DST), Government of India, for providing research support through the "INSPIRE Faculty Award" (IFA12-ENG-09).

[1]G. Zhang and X. W. Lou, Sci. Rep. **3**, 1470 (2013).
[2]P. Simon and Y. Gogotsi, Nature Mater. **7**, 845 (2008).
[3]G. Guo, L. Huang, Q. Chang, L. Ji, Y. Liu, Y. Xie, W. Shi, and N. Jia, Appl. Phys. Lett. **99**, 083111 (2011).
[4]J. Du, G. Zhou, H. Zhang, C. Cheng, J. Ma, W. Wei, L. Chen, and T. Wang, ACS Appl. Mater. Interfaces **5**, 7405 (2013).
[5]F. Yang, J. Yao, F. Liu, H. He, M. Zhou, P. Xiao, and Y. Zhang, J. Mater. Chem. A **1**, 594 (2013).
[6]G. Hu, C. Tang, C. Li, H. Li, Y. Wang, and H. Gong, J. Electrochem. Soc. **158**, A695 (2011).
[7]K. Liang, X. Tang, and W. Hu, J. Mater. Chem. **22**, 11062 (2012).
[8]M. Yang, J. X. Li, H. H. Li, L. W. Su, J. P. Wei, and Z. Zhou, Phys. Chem. Chem. Phys. **14**, 11048 (2012).
[9]C. Yuan, X. Zhang, L. Su, B. Gao, and L. Shen, J. Mater. Chem. **19**, 5772 (2009).
[10]R. B. Rakhi, W. Chen, D. Cha, and H. N. Alshareef, Nano Lett. **12**, 2559 (2012).
[11]L. Yang, S. Cheng, Y. Ding, X. Zhu, Z. L. Wang, and M. Liu, Nano Lett. **12**, 321 (2012).
[12]G. Q. Zhang, H. B. Wu, H. E. Hoster, M. B. Chan-Park, and X. W. Lou, Energy Environ. Sci. **5**, 9453 (2012).
[13]H. Jiang, J. Mab, and C. Li, Chem. Commun. **48**, 4465 (2012).
[14]H. Wang, Q. Gao, and L. Jiang, Small **7**, 2454 (2011).
[15]A. K. Singh, D. Sarkar, G. G. Khan, and K. Mandal, J. Mater. Chem. A **1**, 12759 (2013).
[16]See supplementary material at http://dx.doi.org/10.1063/1.4870628 for the details of the fabrication and characterization of Co-Ni/Co_3O_4-NiO core/shell nano-heterostructures electrode.
[17]J. H. Kim, K. Zhu, Y. Yan, C. L. Perkins, and A. J. Frank, Nano Lett. **10**, 4099 (2010).
[18]X. Tian, C. Cheng, L. Qian, B. Zheng, H. Yuan, S. Xie, D. Xiao, and M. M. F. Choi, J. Mater. Chem. **22**, 8029 (2012).
[19]C. Yuan, J. Li, L. Hou, X. Zhang, L. Shen, and X. W. Lou, Adv. Funct. Mater. **22**, 4592 (2012).
[20]B. Wang, J. S. Chen, Z. Wang, S. Madhavi, and X. W. Lou, Adv. Energy Mater. **2**, 1188 (2012).
[21]H. L. Wang, H. S. Casalongue, Y. Y. Liang, and H. J. Dai, J. Am. Chem. Soc. **132**, 7472 (2010).
[22]X. H. Xia, J. P. Tu, Y. J. Mai, X. L. Wang, and C. D. Gu, J. Mater. Chem. **21**, 9319 (2011).
[23]J. Jiang, J. P. Liu, R. M. Ding, J. H. Zhu, Y. Y. Li, A. Z. Hu, X. Li, and X. T. Huang, ACS Appl. Mater. Interfaces **3**, 99 (2011).